 doi: 10.2176/jns-nmc.2022-0038

NMC Case Report Journal 9, 199-208, 2022

Genetic Alteration May Proceed with a Histological Change in Glioblastoma: A Report from Initially Diagnosed as Nontumor Lesion Cases

Hayato TAKEUCHI,[1] Yoshinobu TAKAHASHI,[1] Seisuke TANIGAWA,[1] Takanari OKAMOTO,[1] Yoshinori KODAMA,[2] Yukiko SHISHIDO-HARA,[3] Ema YOSHIOKA,[4] Tomoko SHOFUDA,[4] Yonehiro KANEMURA,[4] Eiichi KONISHI,[5] and Naoya HASHIMOTO[1]

[1]*Department of Neurosurgery, Kyoto Prefectural University Graduate School of Medical Science, Kyoto, Kyoto, Japan*
[2]*Division of Pathology Network, Kobe University Graduate School of Medicine, Kobe, Hyogo, Japan*
[3]*Department of Pathology and Applied Neurobiology, Kyoto Prefectural University Graduate School of Medical Science, Kyoto, Kyoto, Japan*
[4]*Department of Biomedical Research and Innovation, Institute for Clinical Research, National Hospital Organization Osaka National Hospital, Osaka, Osaka, Japan*
[5]*Department of Pathology, Kyoto Prefectural University Graduate School of Medical Science, Kyoto, Kyoto, Japan*

Abstract

Despite recent signs of progress in diagnostic radiology, it is quite rare that a glioblastoma (GBM) is detected asymptomatically. We describe two patients with asymptomatic nonenhancing GBMs that were not diagnosed with neoplasia at first. The patients had brain scans as medical checkups, and incidentally lesions were detected. In both cases, surgical specimens histopathologically showed no evidence of neoplasia, whereas molecular genetic findings were isocitrate dehydrogenase (IDH)-wildtype, O^6-methylguanine-DNA methyltransferase promoter (*pMGMT*) unmethylated, and telomerase reverse transcriptase (*TERT*) promoter mutated, which matched to GBM. One patient was observed without adjuvant therapy and the tumor recurred 7 months later. Reoperation was performed, and histopathologically GBM was confirmed with the same molecular diagnosis as the first surgical specimen. Another patient was carefully observed, and chemoradiotherapy was begun 6 months after the operation following the extension of the lesion. Eventually, because of disease progression, both patients deceased. We postulate that in each case, the tumor was not lower-grade glioma but corresponded to the early growth phase of GBM cells. Thus far, cases of malignant transformation from lower-grade glioma or asymptomatic GBM with typical histologic features are reported. Nevertheless, to the best of our knowledge, no such case of nonenhancing, nonhistologically confirmed GBM was reported. We conjecture these cases shed light on the yet unknown natural history of GBM. GBM can take the form of radiological nonenhancing and histological nonneoplastic fashion before typical morphology. Molecular genetic analysis can diagnose atypical preceding GBM, and we recommend early surgical removal and adjuvant treatment.

Keywords: asymptomatic glioblastoma, nonenhancing glioblastoma, IDH-wildtype, TERT mutated

Introduction

Glioblastoma (GBM), the most common malignant brain tumor, bears a dismal prognosis with a median survival of 14.6 months from diagnosis.[1)] When the tumor is smaller, it is more amenable to maximal safe resection. The higher the removal rate is the better the prognosis.[2,3)] Hence, early detection of GBM is an attractive approach to obtaining a

Received February 10, 2022; Accepted May 2, 2022

better prognosis. Despite the recent advancement in diagnostic radiology, however, almost all GBMs are diagnosed when the tumors become symptomatic and their sizes are as large as 40 mm in diameter of the enhanced lesion.[2,3] One of the possible reasons for it could be that unlike many other cancers, the natural history of early GBM remains fully unproven. The origin of GBM has long been debated but is still unsettled. We present two cases of asymptomatic nonenhancing GBMs, each of them was detected incidentally by medical checkups. In both cases, molecular profiles of the surgical specimen corresponded to GBM, but histologically neoplastic change could not be detected. After months of observation, a huge enhancing mass lesion was detected in the first case, and a ring-enhancing lesion emerged despite chemoradiotherapy in the second case.

Materials and Methods

Study design and patients

The patients were having brain magnetic resonance (MR) images for medical checkups periodically. They were asymptomatic and healthy when preceding lesions were detected. This study was approved by the Institutional Review Board of Kyoto Prefectural University Graduate School of Medical Science (ERB-C-2048), and written informed consent was obtained from all patients.

Neuroradiological examinations

Standard MR imaging protocol including T1-weighted image (T1WI) with or without gadolinium (Gd) enhancement, T2-weighted image (T2WI), and fluid-attenuated inversion recovery (FLAIR) was routinely studied. Additionally, before each surgery, perfusion images to measure regional cerebral blood flow/volume (rCBF/rCBV) were studied. All MR imaging examinations were obtained using a 1.5-Tesla whole-body imager (Philips Medical Systems, Best, The Netherlands).

Histopathological and molecular examinations

Tumor tissues obtained from surgery were divided into half and provided for histopathological and molecular examinations. For histopathological examinations, tumor samples were formalin fixed immediately, then embedded in paraffin, and thin sliced at 5 μm thickness. Sections were then stained with hematoxylin-eosin using standard protocols. Immunohistochemistry was also performed using standard procedures, with primary antibodies as described below: p53 (mouse monoclonal, Nichirei Biosciences, Tokyo, Japan), ATRX (rabbit polyclonal, Atlas Antibodies, Stockholm, Sweden), GFAP (rabbit monoclonal, Cell Marque, Rocklin, CA), IDH1 R132H (mouse monoclonal, dianova, Germany), Ki-67 (mouse monoclonal, Dako, Glostrup, Denmark). For molecular investigation hotspot mutations of IDH1/2 (codon 132 of *IDH1* and codon 172 of *IDH2*) and the *TERT* promoter (*pTERT*, termed C228 and C250) were assessed using Sanger sequencing. The methylation status of the O^6-methylguanine-DNA methyltransferase promoter (*pMGMT*) was analyzed and assessed by quantitative methylation-specific PCR after bisulfite modification of DNA extracted from tissue.[4] Allele frequency of tumor genome DNAs containing *pTERT* mutations was estimated from the peak height of signals using Sanger sequencing data. C228T allele was also confirmed using SNP Genotyping assay by QuantStudio 3D Digital ProFlex PCR system (Thermo Fisher Scientific, Carlsbad, CA, USA) according to the manufactures instruction. When the molecular examination revealed IDH-wildtype, H3-wildtype, and *pTERT* mutated, we assigned that the tumor has the molecular GBM signature.[5]

Adjuvant treatments

For adjuvant treatment, Stupp's regimen including regional irradiation with a total of 60 Gy in 30 fractions with concomitant temozolomide (TMZ, 75 mg/m^2 daily for 6 weeks), followed by a maintenance chemotherapy with a 4-week course of TMZ (150 mg/m^2 daily for 5 days in the initial cycle and then dose up to 200 mg/m^2 for further cycles), was applied. When necessary, 15 mg/kg of bevacizumab every 3 weeks was added.

Case Presentation

Case 1: A 58-year-old right-handed woman, whose MR imaging was normal 10 years ago (Fig. 1A), was referred to our institution because of a hyperintense lesion on T2-weighted MR images in the right mesial temporal lobe and amygdala detected incidentally (Fig. 1B). She had undergone a plain MR imaging scan as medical checkups and was asymptomatic and neurologically intact. She had no medical history at the initial MR scan, and during the decade, she did not experience seizure attacks, stroke, head trauma, or other cerebral diseases. This time, the lesion was poorly circumscribed, with isointensity on T1WI and hyperintensity on T2WI. Further investigation revealed that it was nonenhancing by Gd and showed no significant elevation of rCBF (Fig. 1C-F). Angiography indicated no cerebrovascular abnormality, and ^{18}F-fluorodoexy glucose-positron emission tomography displayed no uptake (figure not shown). From these results, lower-grade glioma (LGG) was suspected, and we recommended her to have the tumor removed. Eight months later, in which a follow-up scan showed no remarkable aggravation of the lesion, the operation was performed. Via a right frontotemporal craniotomy, with an aid of neuronavigation, a partial temporal lobectomy for removal of the lesion was achieved. The color and hardness of the lesion were indistinguishable macroscopically from the normal brain. Removal of the hyperintensity area on T2WI was confirmed via immediate postoperative MR imaging (Fig. 1G). Histopathologically,

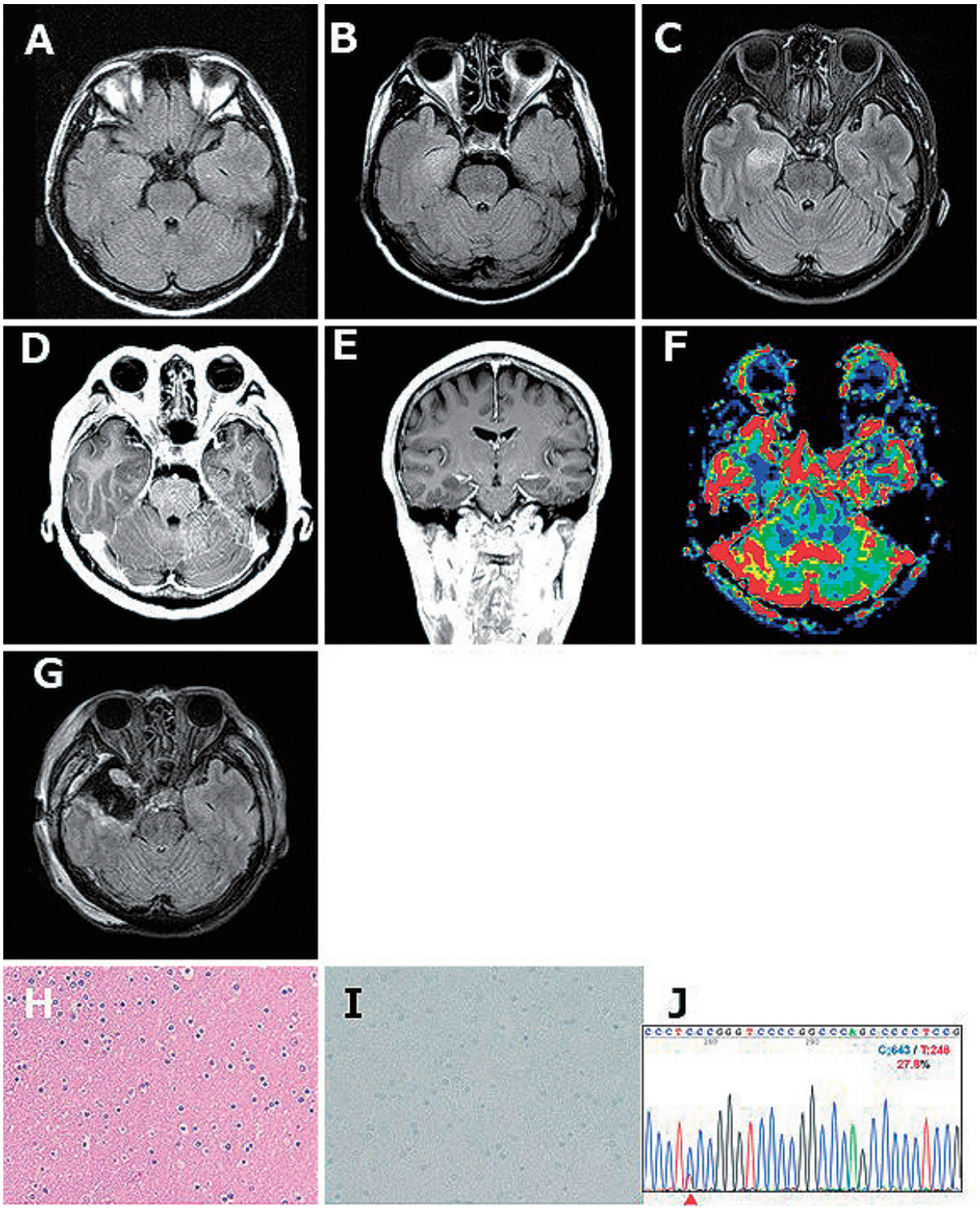

Fig. 1 Initial radiological and histopathological images of Case 1. Magnetic resonance (MR) images of the patient studied for medical checkups (A, B). Axial FLAIR image obtained 10 years before when the patient was 48 years old shows no abnormality (A). Axial FLAIR scan at this time showing a hyperintensity lesion in the right hippocampus and uncus (B). MR images taken 4 months after the discovery of the right hippocampal lesion. Axial FLAIR image (C), axial Gd-enhanced T1-weighted image (D), and coronal Gd-enhanced T1-weighted image (E) indicating no enhancement of the hippocampus. Perfusion-weighted axial image showing no aggregation of cerebral blood flow (F). A postoperative FLAIR image indicating removal area containing almost the whole area of the lesion (G). Hematoxylin and eosin staining (H) showing no proliferation of atypical cells. Immunohistochemical staining for Ki-67 (I), original magnification: ×40. A result of Sanger sequencing of the specimen (J), showing 27.8% had C250T TERT promoter mutation.

the specimen showed normocellularity, and there was no evidence of atypical cells, indicating nonneoplastic features (Fig. 1H). Immunohistochemically, no positive cells for Ki-67 (Fig. 1I) and p53 were found. Thus, no tumor lesion could be identified in histological examination. The result of the molecular investigation was IDH-wildtype, H3-wildtype, and *pTERT* mutated (Fig. 1J) (molecular GBM signature), and *pMGMT* unmethylated. Because the MR imaging findings had not changed during 8 months of follow-up and the histopathological diagnosis could not show neoplastic transformation, no adjuvant therapy such as irradiation or chemotherapy was planned. The patient was discharged home without any neurological deficit. We offered close observation with repeat MR images, but a few months after the operation, she canceled the clinic visit and was lost to follow-up. Seven months after the surgery (15 months from the initial scan), she came to our emergency room complaining of general fatigue, headache, and nausea. MR images revealed a massive large enhanced mass with high blood flow that had a maximum diameter of 45 mm located in the previous surgical cavity (Fig. 2A-C). Two days later, reoperation for subtotal removal of the lesion was performed. Postoperatively, her symptoms improved swiftly. This time, a histopathological diagnosis of GBM was made because necrosis, microvascular proliferation, and atypical cells were evident (Fig. 2D-F). Immunohistochemically Ki-67 labeling index was approximately 15% (Fig. 2G), p53 was positive for only a few tumor cells (Fig. 2H), IDH1 (R132H) was negative (Fig. 2I), ATRX was positive (retained) (Fig. 2J), and GFAP was positive (figure not shown). Molecular analysis again revealed a molecular GBM signature that was completely the same as the initial one: IDH-wildtype, H3-wildtype, *pTERT* mutated (Fig. 2K), and *pMGMT* unmethylated. After the second operation, adjuvant therapy according to Stupp's regimen was carried out, but tumor recurrence was confirmed 17 months after the first operation, until when five courses of maintenance TMZ had been administered. During the course, bevacizumab was added, and the patient deteriorated and deceased 26 months after the first operation.

Case 2: This 50-year-old right-handed woman annually underwent MR imaging as a medical checkup since the FLAIR image detected multiple hyperintensity lesions in the deep white matter 8 years ago (Fig. 3A). The white matter lesions were asymptomatic, and the FLAIR image remain unremarkable until a year ago (Fig. 3B). Nevertheless, this time aggregation of the T2WI/FLAIR hyperintensity area developed in the left frontal white matter (Fig. 3C, arrowheads). Additional imaging showed the lesion was slightly hypointensity in T1WI and was not enhanced with Gd (Fig. 3D and E). She underwent awake surgery to resect the lesion. The correctness of the surgical removal of the lesion was confirmed by postoperative MR images (Fig. 3F and G). The histopathological study showed that slightly higher cellularity mainly with reactive astrocytes or infiltration of histiocytes was observed, indicating the existence of inflammation. On immunohistochemical analysis, those cells were positive for ATRX, and negative for IDH1 (R132H) and p53, and the Ki-67 labeling index was 0.8% (Fig. 3H-L). Thus, cell proliferation was interpreted not as neoplastic change but rather as reactive gliosis. In the molecular diagnosis, molecular GBM signature, IDH-wildtype, H3-wildtype, and *pTERT* mutated (Fig. 3M), and unmethylated *pMGMT*, was detected. Despite this discrepancy between histopathological and molecular results, we assumed the possibility of GBM-like behavior of the lesion, and we began a close observation with monthly MR studies. Five months after the operation, elongation of the T2WI hyperintensity tail toward the corpus callosum was detected (Fig. 3F and G). Consequently, we have advised chemoradiotherapy, and at that moment, she did not show any neurological manifestation. Treatment according to Stupp's regimen was started 7 months after the surgery. However, during maintenance chemotherapy with TMZ, she got progressive cognitive decline and MR images obtained 10 months after the operation revealed a ring-enhancing lesion in the left frontal lobe (Fig. 3N and O). A proposal to re-operate for removal of the mass lesion was not realized by refusal from the patient and the family. Eventually, her symptom exacerbated and chemotherapy was abandoned after three courses of TMZ, and then, she passed away 12 months after the operation.

Discussion

We have reported cases in which "nonspecific" lesions both from neuroradiological and histopathological points of view progressed into massive GBM in just a couple of months (Supplementary Figure). These tumors would be interpreted as two kinds of disease course: very early growth phase of GBM and progression of LGG to GBM. We assume these cases were the former, not the latter. We also assume that these cases would be a corroboration of the ultra-early growth phase of GBM, which traditional diagnostic modalities cannot detect. With compelling data, diagnosis of GBM, IDH-wildtype will be made when an IDH-wildtype diffuse and astrocytic glioma have either of microvascular proliferation, necrosis, *pTERT* mutation, *EGFR* gene amplification, or +7/−10 chromosome copy number changes.[5] These molecular changes (*pTERT* mutation, *EGFR* gene amplification, and +7/−10 chromosome copy number changes) are called "molecular GBM signature." Even when the tumor histologically shows benign features that for example lack necrosis or microvascular proliferation, the existence of one or more molecular GBM signatures is enough to diagnose GBM. In that case, the tumor contains features of diffuse astrocytoma such as increased cellularity and nuclear atypia. Compared with that, the cases here showed no such glioma-like characteristics; in both cases, there could not be found atypical cells, and in

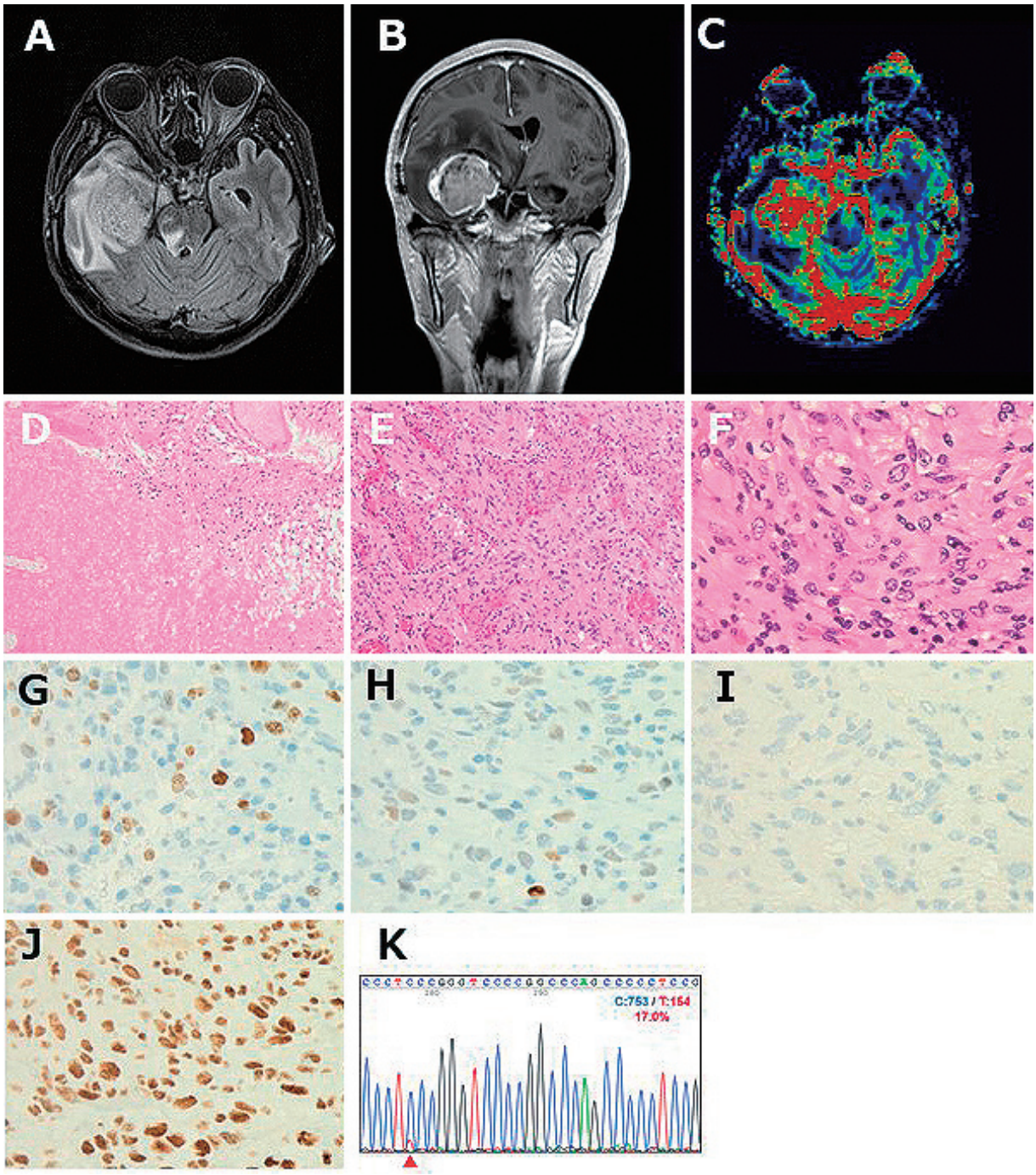

Fig. 2 Radiological and histopathological images after the recurrence of Case 1. An axial FLAIR (A) and coronal Gd-enhanced image (B) showing solid enhanced mass, typical findings of GBM just the same place as the removed lesion at the initial operation. Perfusion image (C) showing elevated blood flow. Hematoxylin and eosin staining showing necrosis (D), microvascular proliferation (E), and proliferation of atypical cells (F), original magnification: ×10 (D, E), ×40 (F). Immunohistochemical staining for Ki-67 (G), p53 (H), IDH1 (R132H) (I), ATRX (J), original magnification: ×40. A result of Sanger sequencing of the specimen (K), showing 17.0% had C250T TERT promoter mutation.

Case 1, the cellularity was almost normal and in Case 2, somewhat higher cellularity was due to infiltration of reactive astrocytes or histiocytes. Additionally, clinically, symptoms deteriorated more rapidly. One could argue that histological diagnosis was made based on incorrectly sampled tissue from a normal brain. However, for the following reasons, it is indisputable that the samples were indeed taken from the core of the tumors themselves; first, the accuracy

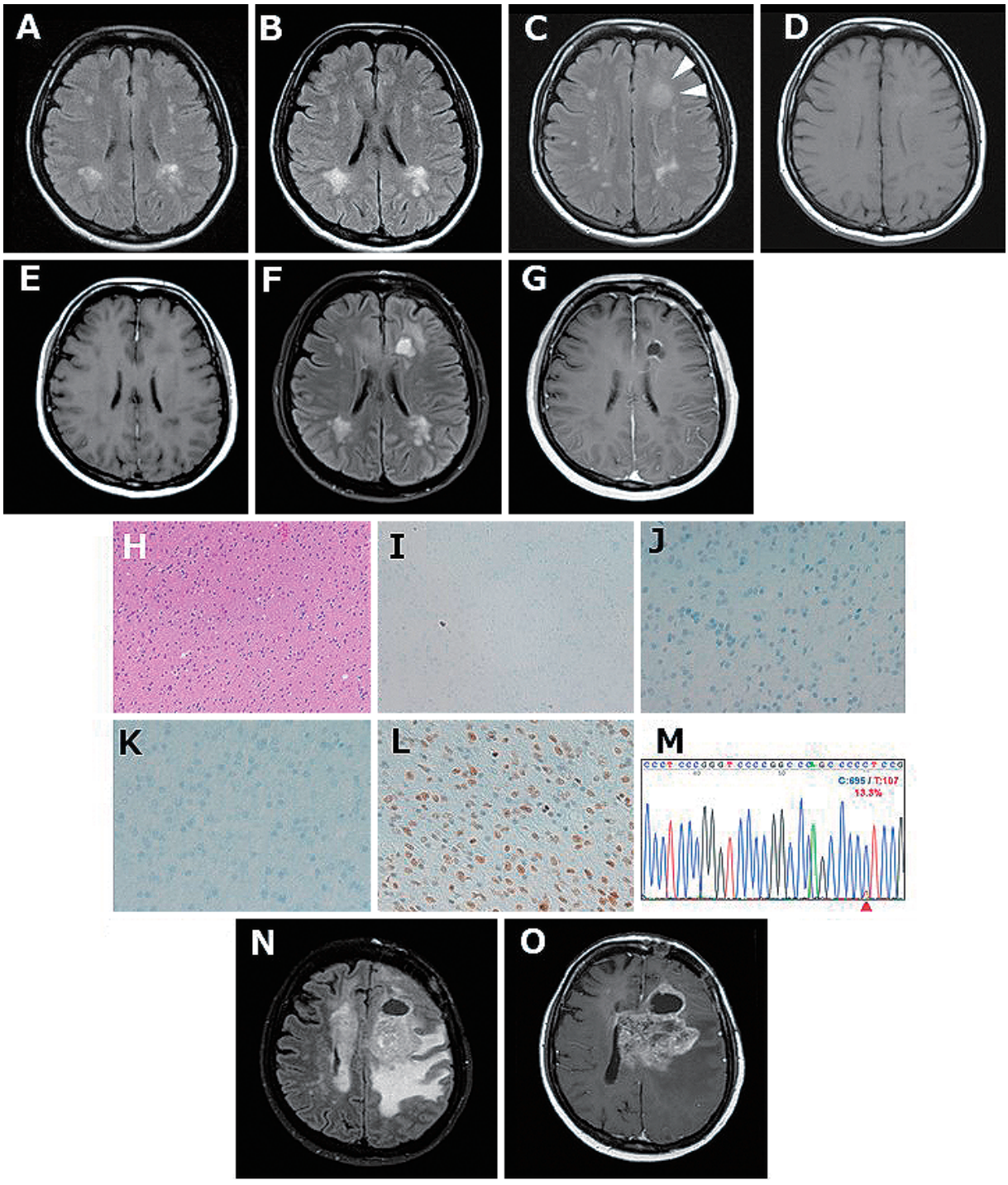

Fig. 3 Radiological and histopathological images of Case 2. An MR image taken 8 years before showing multiple deep white matter hyperintensity (A). An MR image taken 1 year before also showing deep white matter hyperintensity (B). MR images showing the emergence of T2WI hyperintensity lesion in the left frontal white matter (C, arrowhead) that are hypointensity in T1WI (D) and not enhanced with Gd (E). MR images 3 months after the operation indicating that the hyperintensity area was elongating toward the corpus callosum (F) but was not enhanced with Gd (G). Note that the removal cavity of the operation is seen in exactly the same loci of the T2WI hyperintensity lesion in C. Histopathological findings indicating a slight increase in cell density in HE (H), and scarce positive cells for Ki-67 staining (I), and negative for p53 (J) and IDH1 (R132H) (K), and positive for ATRX (L). Original magnification: ×20 (H, I), ×40 (J, K, L). A result of Sanger sequencing of the specimen (M), showing 13.3% had C228T TERT promoter mutation. Radiological images after disease progression of Case 2. Ten months after the operation, images revealed a massive enhanced lesion next to the operative cavity (N, O).

Table 1 Reported cases of non-conclusive lesions that turned out to be GBMs

author, year	age	sex	symptom	location	initial MR study	initial surgical findings	interval between initial imaging and diagnostic operation	second MR study	final diagnosis	IDH status
Landy et al. 2000 [7]	58	M	seizure	N/D	negative		8 m	N/D	GBM	N/D
	40	F	seizure	N/D	negative		3.25 m	N/D	GBM	N/D
	71	M	seizure	N/D	negative		2 m	N/D	GBM	N/D
Okamoto et al. 2002 [8]	38	M	dysesthesia	lt parietal white matter	T1 HI		10 m	cystic lesion	GBM	N/D
Cohen-Gadol et al. 2004 [9]	40	M	seizure	right frontal	T2 HI	AA	17 w	ring enhancement	GBM	N/D
	68	M	seizure	right medial temporal lobe	T2 HI		16 w	ring enhamcement	GBM	N/D
Jung et al. 2007 [10]	63	F	headache, left hemi-paresis	rt temporofronto-parietal	T2 HI		6 m	ring enhancement	GBM	N/D
	54	M	seizure	lt occipital	T2 HI		6 m	ring enhancement	GBM	N/D
Nishi et al. 2009 [11]	68	M	seizure	lt temporal	normal		3 m	cystic lesion	GBM	N/D
	50	M	seizure	lt frontal	normal		5 m	N/D	GBM	N/D
	53	M	seizure	lt temporal	normal		3 m	ring enhancement	GBM	N/D
	65	M	dizziness	lt temporal	T2 HI		4 m	N/D	GBM	N/D
	65	M	seizure	lt frontal	T2 HI		3 m	N/D	GBM	N/D
Oyama et al. 2010 [12]	73	M	hemiparesis	lt frontal	DWI, T2 HI		7 w	ring enhancement	GBM	N/D
Rossi et al. 2010 [13]	68	F	seizure	rt temporal	T2 HI		2 m	ring enhancement	GBM	N/D
Nam et al. 2011 [14]	70	M	cognitive impair-ment, fever, headache	lt medial tempo-ral lobe	T2 HI		8 m	ring enhancement	GBM	N/D
Takagi et al. 2011 [15]	57	F	seizure	rt insula	T2 HI	abondoned	4 m	ring enhancement	GBM	N/D
Thaler et al. 2012 [16]	80	F	seizure	N/D	negative		3.3 m	enhancement	GBM	N/D
	77	M	weakness	N/D	negative		20.2 m	ring enhancement	GBM	N/D
	38	F	seizure	N/D	negative		5.1 m	N/D	GBM	N/D
	56	F	seizure	N/D	negative		76.6 m	N/D	GBM	N/D
	90	M	memory loss	N/D	negative		4.5 m	enhancement	GBM	N/D
	77	F	seizure	N/D	T2 HI		1.5 m	N/D	GBM	N/D
	64	M	seizure	N/D	T2 HI		1.1 m	enhancement	GBM	N/D
	47	M	seizure	N/D	T2 HI		2.9 m	ring enhancement	GBM	N/D
	64	M	seizure	N/D	T2 HI		2.0 m	N/D	GBM	N/D
	73	F	seizure	N/D	T2 HI		2.2 m	N/D	GBM	N/D
	59	M	seizure	N/D	T2 HI		1.6 m	N/D	GBM	N/D
	71	F	seizure	N/D	T2 HI		0.7 m	N/D	GBM	N/D

Table 1 Reported cases of non-conclusive lesions that turned out to be GBMs (continued)

author, year	age	sex	symptom	location	initial MR study	initial surgical findings	interval between initial imaging and diagnostic operation	second MR study	final diagnosis	IDH status
Ideguchi et al. 2015 [17]	63	F	none	lt occipital	T2 HI		2.9 m	heterogenous enhancing	GBM	wt
	63	F	left hemiparesis	rt parietal	T2 HI		2.5 m	heterogenous enhancing	GBM	wt
	70	M	headache	lt frontal	T2 HI		5.9 m	ring enhancement	GBM	wt
	54	F	none	rt temporal	T2 HI		3.4 m	ring enhancement	GBM	wt
Toh et al. 2017 [18]	55	M	seizure	rt insula and temporal cortex	T2 HI		11 m	N/D	GBM	wt
	57	M	seizure	lt parietal cortex	T2 HI		7 m	N/D	GBM	mut
	60	M	seizure	rt insula and frontal operculum	T2 HI		8 m	N/D	GBM	wt
	48	M	LOC	lt temporal	T2 HI		12 m	N/D	GBM	wt
	40	F	syncope	rt insula and frontal operculum	T2 HI		11 m	N/D	GBM	N/D
	32	F	speech	lt parietal	T2 HI		4 m	N/D	GBM	wt
	33	M	headache, LOC	rt insula	T2 HI		4 m	N/D	GBM	N/D
	58	F	gait disturbance, memory impairment	rt medial frontal	T2 HI		13 m	N/D	GBM	N/D
	48	M	seizure	rt parietal	T2 HI		10 m	N/D	GBM	mut
	78	F	headache	rt temporal	T2 HI		2 m	N/D	GBM	wt
	41	M	seizure	lt temporal	T2 HI		1.5 m	N/D	GBM	wt
	40	M	seizure	lt parietal	T2 HI	GBM		N/D		N/D
	71	M	visual TIA	rt occipital	T2 HI		2 m	N/D	GBM	N/D
	27	M	seizure	lt frontal	T2 HI	GBM		N/D		mut
Present Case	58	F	none	right uncus	T2 HI	non-neoplastic	16 m	ring enhancement	GBM	wt
	50	F	none	lt frontal	T2 HI	non-neoplastic	3 m	ring enhancement	GBM	wt

HI: hyperintense area, m: month (s), mut: mutant, w: weeks, wt: wildtype

of location was proven by the usage of neuronavigation and postoperative MR images. Second, each specimen provided for histological diagnosis came from the same sample that was used for molecular diagnosis. Third, although the Ki-67 labeling index was low, we think GBM cells not in division cycle were included. By molecular analysis, the same sample revealed wildtype IDH and mutated *pTERT*, which corresponds to GBM. We did not analyze *EGFR* amplification and chromosomal changes, but as the result of the recent study indicates, analysis of *pTERT* mutation status is sufficient to diagnose GBM, *IDH*-wildtype.[6] As the high signal of *pTERT* mutation might explain the higher tumor cell ratio, the results of the cases indicate only a small percentage (27.8% and 13.3%, respectively) of the tissue containing GBM cells. Unexpectedly, in Case 1, the signal in recurrence (17.0%) was lower than the initial. The possible reasons for this, we guess, are the heterogeneous nature of glioma affected as intratumoral dispersion or necrotic tissue in the recurrence reduced the intensity of the signal. We also speculate that it needs an accumulation of similar cases for a detailed discussion of this phenomenon. As far as we know, there are 48 cases of GBMs first defined as "nondiagnostic" or "normal image" by MR images (Table 1).[7-18] Most of them were discovered by seizure attack and consequently demonstrate typical GBM findings such as ring-like enhancement in a median of 5 months. Some were operated on in the nonenhancing period and histological diagnosis turned out to be LGG or GBM. In our cases, the patients were asymptomatic, and we performed surgical removal 7-10 months before the tumor showed a typical radiological GBM appearance. Additionally, histopathological findings were without evidence of a tumor. By investigating 16 cases of nonenhancing lesions that rapidly progressed to GBM, Toh and colleagues mentioned that these lesions were not low-grade gliomas but high grade from their origin.[18] There also is a reported case of nonenhancing lesions distant from histologically proven GBMs.[19]

In Japan, the number of MR imaging units is approximately 60 per million population, which is the highest number in the world.[20] To make use of it, healthy or asymptomatic people often have an MR imaging scan of the brain for medical checkups. On some occasions, unruptured aneurysms or small meningiomas are detected, but only 2% of GBM is diagnosed asymptomatically.[21] One reason for the scant asymptomatic GBM is that the very early stage of GBM progression is not fully recognized. The cell of origin of GBM is discussed but not solved so far. Recently, a report proved that in *IDH*-wildtype GBM, the founder cell emerges approximately 2-7 years before diagnosis and undergoes several years of evolution before being detected.[22] Another report demonstrated that GBM arises from the subventricular zone (SVZ) cells and migrates to the cerebral cortex and develops into GBM.[23] Additionally, the findings of monoclonal multicentric GBM show that the existence of GBM cells is not visible on the MR images and migration from SVZ is speculated.[24] Taken together, founder cells of GBM arise from SVZ cells years before the onset, and then migrate to the tumor location, which cannot be detected by current neuroimaging techniques. Based on this hypothesis, our cases correspond to the early growth phase of GBM cells. In Case 1, as the remaining tumor of 4 mm in the diameter grew up to 4 cm mass in the next 7 months, by our calculation, the cell doubling time was 20 days. Based on reports GBM's cell division rate was approximately once in 10-49.6 days.[21,25,26] To our knowledge, therefore, these are the first cases in which an early growth phase of GBM cells was identified wherein the lesion was neuroradiologically and histopathologically nonspecific.

Conclusion

We have detected GBMs in the very early growth phase in two cases, which previously might have been thought of as indeterminate lesions. As we have experienced, even when conventional modalities cannot detect neoplastic change, molecular profile clearly indicate GBM nature antecedent to radiological or histological manifestation. Thanks to the progress of molecular biology, we now can decide these cases as GBM, *IDH*-wildtype. These cases may be a help to understand the natural history of yet unknown early phase of GBM. Neuropathologists and neurosurgeons should be aware of the existence of nonenhancing early phase of GBM. Additionally, early therapeutic intervention based on molecular diagnosis shall be considered.

Supplementary Material

https://doi.org/10.2176/jns-nmc.2022-0038

Author Contributions

Conception and design: HT. Data collection: HT, YT, TO, and NH. Data analysis: ST, YKo, YSH, EK, EY, TS, and NH. Manuscript writing, revision, and completion: HT, YKo, YKa, YSH, and NH. All authors read and approved the final manuscript.

Funding Information

The authors did not receive support from any organization for the submitted work.

Conflicts of Interest Disclosure

The authors report no conflicts of interest pertinent to this manuscript.

References

1) Stupp R, Taillibert S, Kanner A, et al.: Effect of tumor-treating fields plus maintenance temozolomide vs maintenance temozolomide alone on survival in patients with glioblastoma a randomized clinical trial. *JAMA* 318: 2306-2316, 2017
2) Lacroix M, Abi-Said D, Fourney DR, et al.: A multivariate analysis of 416 patients with glioblastoma multiforme: prognosis, extent of resection, and survival. *J Neurosurg* 95: 190-198, 2001
3) Sanai N, Polley M-Y, McDermott MW, Parsa AT, Berger MS: An extent of resection threshold for newly diagnosed glioblastomas. *J Neurosurg* 115: 3-8, 2011
4) Umehara T, Arita H, Yoshioka E, et al.: Distribution differences in prognostic copy number alteration profiles in IDH-wild-type glioblastoma cause survival discrepancies across cohorts. *Acta Neuropathol Commun* 7: 99, 2019
5) Louis DN, Aldape KD, Capper D, et al.: Glioblastoma, IDH-wildtype, in Brat DJ, Ellison DW, Figarella-Branger D, et al. (eds): WHO classification of tumours of the central nervous system. Lyon, International Agency for Research on Cancer, 2021, pp 39-55
6) Fujimoto K, Arita H, Satomi K, et al.: TERT promoter mutation status is necessary and sufficient to diagnose IDH-wildtype diffuse astrocytic glioma with molecular features of glioblastoma. *Acta Neuropathol* 142: 323-338, 2021
7) Landy HJ, Lee TT, Potter P, Feun L, Markoe A: Early MRI findings in high grade glioma. *J Neurooncol* 47: 65-72, 2000
8) Okamoto K, Ito J, Takahashi N, et al.: MRI high-grade astrocytic tumors: early appearance and evolution. *Neuroradiology* 44: 395-402, 2002
9) Cohen-Gadol AA, DiLuna ML, Bannykh SI, Piepmeier JM, Spencer DD: Non-enhancing de novo glioblastoma: report of two cases. *Neurosurg Rev* 27: 281-285, 2004
10) Jung TY, Jung S: Early neuroimaging findings of glioblastoma mimicking non-neoplastic cerebral lesion—two case reports. *Neurol Med Chir (Tokyo)* 47: 424-427, 2007
11) Nishi N, Kawai S, Yonezawa T, Fujimoto K, Masui K: Early appearance of high grade glioma on magnetic resonance imaging. *Neurol Med Chir (Tokyo)* 49: 8-12, 2009
12) Oyama H, Ando Y, Aoki S, et al.: Glioblastoma detected at the initial stage in its developmental process—case report. *Neurol Med Chir (Tokyo)* 50: 414-417, 2010
13) Rossi R, Figus A, Corraine S: Early presentation of de novo high grade glioma with epileptic seizures: electroclinical and neuroimaging findings. *Seizure* 19: 470-474, 2010
14) Nam TS, Choi KH, Kim MK, Cho KH: Glioblastoma mimicking herpes simplex encephalitis. *J Korean Neurosurg Soc* 50: 119-122, 2011
15) Takagi I, Shakur SF, Lukas RV, Eller TW: Spontaneous radiographic resolution and subsequent redemonstration of an untreated glioblastoma: case report. *J Neurosurg* 115: 24-29, 2011
16) Thaler PB, Li JY, Isakov Y, et al.: Normal or non-diagnostic neuroimaging studies prior to the detection of malignant primary brain tumors. *J Clin Neurosci* 19: 411-414, 2012
17) Ideguchi M, Kajiwara K, Goto H, et al.: MRI findings and pathological features in early-stage glioblastoma. *J Neurooncol* 123: 289-297, 2015
18) Toh CH, Castillo M: Early-stage glioblastomas: MR imaging-based classification and imaging evidence of progressive growth. *Am J Neuroradiol* 38: 288-293, 2017
19) Lasocki A, Gaillard F, Tacey MA, Drummond KJ, Stuckey SL: The incidence and significance of multicentric noncontrast-enhancing lesions distant from a histologically-proven glioblastoma. *J Neurooncol* 129: 471-478, 2016
20) Lee JH, Lee JE, Kahng JY, et al.: Human glioblastoma arises from subventricular zone cells with low-level driver mutations. *Nature* 560: 243-247, 2018
21) Brain Tumor Registry of Japan (2005-2008). *Neurol Med Chir (Tokyo)* 57: 9-102, 2017
22) Körber V, Yang J, Barah P, et al.: Evolutionary trajectories of IDH WT glioblastomas reveal a common path of early tumorigenesis instigated years ahead of initial diagnosis. *Cancer Cell* 35: 692-704, 2019
23) Organization for economic co-operation and development: Healthcare resources, Medical technology, Magnetic Resonance Imaging units, total. https://stats.oecd.org/index.aspx?DataSetCode=HEALTH_STAT (Accessed Feb 10 2022)
24) Picart T, Le Corre M, Chan-Seng E, Cochereau J, Duffau H: The enigma of multicentric glioblastoma: physiopathogenic hypothesis and discussion about two cases. *Br J Neurosurg* 32: 610-613, 2018
25) Stensjøen AL, Solheim O, Kvistad KA, et al.: Growth dynamics of untreated glioblastomas in vivo. *Neuro Oncol* 17: 1402-1411, 2015
26) Tsuboi K, Yoshii Y, Nakagawa K, Maki Y: Regrowth patterns of supratentorial gliomas: estimation from computed tomographic scans. *Neurosurgery* 19: 946-951, 1986

Corresponding author: Hayato Takeuchi, MD, PhD.
Department of Neurosurgery, Kyoto Prefectural University Graduate School of Medical Science, 465 Kajii-cho Kawaramachi-Hirokoju, Kamigyo-ku, Kyoto, Kyoto 602-8566, Japan.
e-mail: thayato@pop07.odn.ne.jp